HHS Public Access

Author manuscript

Environ Res. Author manuscript; available in PMC 2024 July 29.

Published in final edited form as:

Environ Res. 2023 November 15; 237(Pt 1): 116932. doi:10.1016/j.envres.2023.116932.

Caffeic acid recarbonization: A green chemistry, sustainable carbon nano material platform to intervene in neurodegeneration induced by emerging contaminants

Jyotish Kumar[a], **Sofia A. Delgado**[a], **Hemen Sarma**[b], **Mahesh Narayan**[a,*]

[a] Department of Chemistry and Biochemistry, The University of Texas at El Paso (UTEP), El Paso, TX, 79968, United States

[b] Department of Botany, Bodoland University, Rangalikhata, Deborgaon, Kokrajhar (BTR), Assam, 783370, India

Abstract

Environmental agents such as pesticides, weedicides and herbicides (collectively referred to as pesticides) are associated with the onset and pathogenesis of neurodegenerative disorders such as Parkinson's (PD) and Alzheimer's (AD) diseases. The development of blood-brain barrier (BBB)-penetrating therapeutic candidates to both prevent and treat the aforementioned xenotoxicant-induced neurodegenerative disorders remains an unmet need. Here, we examine whether caffeic-acid based Carbon Quantum Dots (CACQDs) can intervene in pesticide-associated onset and progress of the PD phenotype. Pulse-chase fluorescence analyses revealed that CACQDs intervene in the soluble-to-toxic transformation of the amyloid-forming protein model Hen Egg White Lysozyme (HEWL). The sp2-rich CACQDs also scavenged free radicals, a milestone along the PD trajectory. In-vitro, CACQDs introduced into a human neuroblastoma-derived cell line (SH-SY5Y) demonstrated negligible cytotoxicity up to 5 mg/mL and protected the cell line against oxidative stress-induced neuronal injury induced by the pesticide and potent neurotoxin, paraquat. Our findings suggest that the potentially BBB-penetrating CACQDs derived from caffeic acid hold promise for mitigating neurodegenerative disorders associated with environmental pesticides and xenobiotic neurotoxicants. Importantly, CACQDs sourced from coffee, coupled with their facile synthesis, represent a sustainable, green chemistry platform for generating interventional candidates in neurodegeneration.

* Corresponding author. Department of Chemistry and Biochemistry, UTEP, 500 W. University Ave., El Paso, TX, 79968, United States. hemen@buniv.edu.in (H. Sarma), mnarayan@utep.edu (M. Narayan).

Declaration of competing interest

The authors declare that they have no known competing financial interests or personal relationships that could have appeared to influence the work reported in this paper.

Credit author statement

J.K. and M.N. Investigated, conceptualized and visualized the experiments. J.K designed and performed all the experiments and wrote the original draft. S.A.D. assisted with the experiments. J. K. and M.N. reviewed the data, interpreted the results and wrote the manuscript. H. S. Reviewed and edited the manuscript.

Keywords

Caffeic acid carbon quantum dots; Neurodegeneration; Amyloid fibrils; Pesticides; Soluble-to-toxic; Redox stress

1. Introduction

Neurodegeneration is a prominent Central Nervous System (CNS) disorder and continues to exact burdens on the quality of life and that of associated caregivers (Chitnis and Weiner, 2017; Zhang et al., 2021). Neurodegenerative diseases include Alzheimer's disease (AD), Parkinson's disease, Huntington's disease (HD), systemic amyloidosis, and prion disease(Dugger and Dickson, 2017; Poovaiah et al., 2018a; Lamptey et al., 2022). These heterogeneous diseases arise from familial and idiopathic reasons with protein accumulation, mitochondrial dysfunction, reactive oxygen species elevation, neuronal injury and synaptic loss representing the sequelae of events along the path trajectory to pathology(Singh et al., 2021; Henriquez et al., 2022). To date, there remains a gap in the satisfactory resolution of neurodegenerative disorders with no cure. A key challenge resides in the inability of candidate molecules that have succeeded in experimental and preclinical trials to cross the BBB, a highly selective barrier for all molecules (Kreuter, 2004; Agarwal et al., 2009). As a result, even though several potential drugs have been forwarded for treating neurodegenerative and neurological disorders, less than 1% cross the BBB(Stockwell et al., 2014; Soni et al., 2016). To complicate matters, the BBB hinders the entry of externally injected molecules from the systemic circulation, a crucial step in drug delivery(Suri et al., 2007; Yi et al., 2014). Access to therapeutics is also restricted by membrane transporters requiring a large treatment dose, resulting in side effects(Begley, 2004).

PD and AD are found to occur sporadically in approximately 95% of patients with the gut-brain axis being one of the conduits (Papapetropoulos et al., 2001; Modi et al., 2016). A second mode of non-familial neurodegenerative onset occurs upon chronic exposure to pesticides (Nandipati and Litvan, 2016; Dorsey and Ray, 2023). Toxicants including rotenone, paraquat, the broad-spectrum agricultural organophosphate pesticide chlorpyrifos and drugs of abuse such as methamphetamine and the MPPP byproduct MPTP, are directly responsible for initiating a cascade of cellular events that lead to onset in sporadic neurodegenerative disorders including PD, AD, HD and Amyotrophic Lateral Sclerosis (ALS). They elicit mitochondria-mediated oxidative stress and mitochondrial dysfunction, protein aggregation, ubiquitin-proteasome (UPS) dysregulation and neuroinflammation (Nandipati and Litvan, 2016; Yan et al., 2016). Rotenone, methamphetamine and the MPTP metabolite, MPP+, increase superoxide production and trigger the release of dopamine from vesicular storage, causing the formation of oxidizing metabolites including dopamine quinones and hydrogen peroxide (Scheme 1).

Along with the mycotoxin and complex II inhibitor 3-Nitropropionic acid, these compounds are excitotoxic. They induce the i) production of nitric oxide, ii) provoke apoptosis which results in neuronal degeneration via peroxynitrite formation and, iii) accelerate the aggregation of amyloidogenic proteins including α-synuclein, amyloid β (Aβ)

and mutant Huntingtin protein (mHTT). Cell-death and pathogenesis of the associated neurodegenerative disorder follows(Deshmukh et al., 2012; Nandipati and Litvan, 2016).

Furthermore, evidence demonstrates that workers exposed to paraquat in working environment develop PD(Uversky, 2004). These neurotoxicants induce loss of dopaminergic neurons resulting in a parkinsonian phenotype. Cytotoxicity examination of such toxicants is required for mechanistic understanding of the mode of action and related pathophysiology(Uversky, 2004). Big data analysis also reveals a link between these organochlorines and organophosphates to neurodegenerative disorders like PD, AD and HD(Deshmukh et al., 2012; Yan et al., 2016).

The development of CNMs-based chemically-tunable platforms has found use in applications across biomedicine, renewing efforts to design and develop suitable candidates that can cross the BBB and target neurodegenerative disorders(Xing et al., 2016; Song et al., 2020; Cheng et al., 2022). For example, Carbon Quantum Dots, synthesized from carbon-containing precursors, when suitably chemically functionalized, possess sizes and properties suitable for crossing the BBB and have found use in biomedicine(Sun et al., 2006; Lim et al., 2015). Biofunctionalized carbon nanotubes (CNTs) exhibit excellent structural and mechanical properties and have cell-penetrating abilities(Saito et al., 2009; Hwang et al., 2013; Song et al., 2020). When nanomaterials are used as a delivery system for CNS disorders, their biological properties must be well-understood(Modi et al., 2009; Poovaiah et al., 2018b; Cui et al., 2021; Singh et al., 2021; Zhang et al., 2021). CQDs synthesized from carbon-based natural resources are biocompatible (low cytotoxicity) and are easily tunable to generate tailored physical and chemical properties(Miller, 2002; Kreuter, 2004; Mohanraj et al., 2013; Bai et al., 2021). Ranging in size from 2 to 20 nm, CQDs are amorphous and water-soluble(Janus et al., 2020; Jung et al., 2022). Relatively newly developed, CQDs are chemically stable, highly biocompatible, brightly luminescent and environmentally friendly(Namdari et al., 2017). Besides optical applications, they have found use in biological sensing, bioimaging and nanomedicine(Lim et al., 2014). Furthermore, CQDs are excellent candidates for biomedical applications as they emit fluorescence from UV to the near-infra red (NIR) region(Molaei, 2019). Despite advances in treatment strategies using nanomedicine, the rate of translation into clinically-applicable products is still not remarkable(Bai et al., 2021; Younis et al., 2022). CQDs demand attention for their potential to cross BBB. There is a need to study their cytotoxicity, bioavailability, antioxidant and neuroprotective ability in biological systems(Jung et al., 2020).

Oxidative stress is a key driver in the loss of cholinergic and dopaminergic neurons in AD and PD, respectively(Banerjee et al., 2015; Blesa et al., 2015; Wei et al., 2018). It leads to elevated reactive oxygen species (ROS) originating from genetic mutations or sporadic and idiopathic causals, including exposure to environmental neurotoxins and commercial pesticides(Blesa et al., 2015; Hernandez et al., 2015). In the laboratory, in vitro and in vivo PD models can be generated using paraquat (1,1′-dimethyl-4,4′-bipyridine), a widely used pesticide that recapitulates the cardinal features of PD(Di Monte et al., 2002; Warner et al., 2003; Vaccari et al., 2017). Researchers have employed paraquat due to its potential toxicity to humans and its relation to CNS disorders (Sartori and Vidrio, 2018). Paraquat causes oxidative stress by increasing the superoxide concentration, which is cytotoxic and results in

cell death (Alizadeh et al., 2022). In vitro and in vivo studies show that paraquat can cross BBB from systemic circulation and is toxic to dopaminergic neurons(Corasaniti et al., 1992; McCormack et al., 2005; Miller, 2007).

Caffeic acid is a phenolic acid found in foods such as apples, red wine, and coffee beans(Chen and Ho, 1997; Silva et al., 2014; Monteiro Espíndola et al., 2019). It possesses antioxidant activity and is immunomodulatory and anti-inflammatory(El-Seedi et al., 2012; Mirzaei et al., 2021; Cal et al., 2022). Its presence in the Cerebro Spinal Fluid (CSF) suggests it can cross the BBB(Scalbert et al., 2005; Grabska-Kobylecka et al., 2020). In this study, we have employed caffeic acid as a carbon source for generating and testing CQDs against environmental xenotoxicant-induced PD. The motivation for synthesizing CQDs using caffeic acid as a carbon source is because it is likely that some functional groups in caffeic acid are retained during its recarbonization to form CACQDs, proving advantageous for penetration of the BBB(Alam et al., 2022). CACQDs, in contrast to caffeic acid, have added advantageous for mitigating xenotoxicant-induced neurodegenerative onset because they are likely to possess a richer sp^2-network for radical scavenging and can also be further chemically tuned to improve the BBB-penetrating properties.

We have investigated whether CACQDs can intervene in the soluble-to-toxic transformation of HEWL, model amyloid-forming protein(Mishra et al., 2007). We have also examined whether CACQDs can scavenge free radicals arising from a potent environmental pesticide and neurotoxicant, viz. paraquat. The results of this study suggest that CACQDs should be further tested in vertebrate models of Parkinson’s disease to determine their potential to cross the BBB.

Lastly, caffeic acid and its conversion into CACQDs via the hydrothermal process qualify as both sustainable and green chemistry, making this carbon source particularly attractive in biomedicine(Zhang et al., 2016; Zielińska et al., 2021).

2. Materials and methods

2.1. Chemicals and reagents

Caffeic acid was purchased from Sigma Aldrich USA. HEWL was purchased from Sigma. Thioflavin T, potassium phosphate monobasic and Dibasic (7778–77–0, 7758–11–4), and guanidinium hydrochloride (50–01–1) were purchased from Fisher Scientific. 1,1-diphenyl-2-picryl-hydrazyl (DPPH; Millipore-Sigma USA), methyl viologen dichloride hydrate (paraquat) was purchased from Sigma-Aldrich. All chemicals were of analytical grade and used without further purification. Milli Q (MQ) water was used in all the experiments.

2.2. Cell lines and supplements

Human neuroblastoma-derived SH-SY5Y cells were purchased from ATCC, Manassas, VA, USA. Fetal bovine serum (FBS), penicillin, streptomycin, trypsin (0.25%), DMSO (cell culture grade), DMEM/F-12 (Dulbecco’s Modified Eagle Medium/Nutrient Mixture F-12) were purchased from Sigma-Aldrich. Propidium iodide (PI) Hoechst and trypsin-EDTA

0.25% were purchased from Life Technologies. Penicillin and streptomycin used in this study were obtained from Gibco.

2.3. Synthesis of caffeic acid quantum dots

Caffeic acid carbon quantum dots were synthesized using the one-step hydrothermal method(Yao and Zhao, 2022). Caffeic acid (150 mg) was dissolved in 30 mL MQ water. The solution was subjected to mixing using a magnetic stirrer in an Erlenmeyer flask for a duration of 5 min. The homogenous solution was transferred into a sealed Teflon lined autoclave at 230 °C for 2h. The synthesized CACQDs were cooled to room temperature before centrifugation for 30 min, followed by sonication. The mixture was then filtered with a sterile syringe of pore size 0.22 μm to obtain a transparent brown color solution. The purification of CACQDs solution was performed by dialysis using 1 kDa molecular weight cutoff dialysis tube in MQ water for 10 h against DI water. Purified CACQDS were lyophilized and kept at room temperature. A fresh solution, in the appropriate buffer (see below) was prepared each time from the lyophilized powder for further experiments.

2.4. Physicochemical characterization

The UV–vis absorption spectra of QDs were measured between wavelength of range 200–800 nm. All observations were recorded using the Chemglass Life Sciences SpecMate spectrophotometer. For measurements of the fluorescence intensity and excitation-dependent emission spectra DM45 Olis spectrofluorometer (Online Instrument System, Inc.) was used. For Infrared spectra Thermo Scientific Nicolet iS5 spectrometer was used and measurements were recorded.

2.5. Cell culture

SH-SY5Y Cells were cultured and maintained in a cell culture incubator at 37 °C under 5% carbon dioxide (CO_2). The cell culture medium was DMEM/F12 supplemented with 10% fetal bovine serum (FBS), and 1% penicillin/streptomycin. For cell culture experiments 96-, 24- and 12-well plates were used.

2.6. Fluorescence spectral analysis

The solution of CACQDs with concentration 5 mg/mL was used for fluorescence measurements. A CACQDs stock solution was prepared by introducing a known mass into a pH 7 buffer (20 mM Tris-HCl). The fluorescence spectrum was measured using DM45 Olis spectrofluorometer (Online Instrument System, Inc.). Excitation-dependent emission spectra were obtained upon excitation from 290 nm to 390 nm. All data were processed and plotted using Microsoft Excel and OriginLab (data analysis software) as described elsewhere.

2.7. Dynamic Light Scattering (DLS) and zeta potential measurements

The particle size distribution and surface charge of CACQDs were measured using a Malvern Zetasizer Nano ZS. CACQDs solution in MQ with 50 μL of 5 mg/mL stock solution was diluted to 2 mL in MQ, placed in polystyrene disposable cuvettes, and recorded measurements. For Zeta potential measurements, 100 μL of the same stock was diluted to

1 mL of MQ set in ZETA possible Sample cell Capillary Cuvette DTS1070 was used. Data was processed using Malvern Zetasizer Nano ZS.

2.8. Radical scavenging activity by DPPH method

Briefly, 0.2 mg/mL of DPPH stock solution was prepared in absolute ethanol and kept in the dark at 4 °C. 0.1 mg/mL of ascorbic acid solution was ready for positive control experiments. Similarly, 0.1 mg/mL of CACQDs solution was prepared in methanol from lyophilized powder. By dilution, different concentrations (10 μg/mL to 100 μg/mL) of CACQDs were prepared in absolute ethanol. 4.5 mL of CACQDs solution was kept in separate vials, and 0.5 mL of DPPH solution was added to individual vials to obtain a final volume of 5 mL. When DPPH was added, a color change was observed from violet to yellow, indicating radical scavenging activity of CACQDs compared to the control. All the vials were kept dark for 30 min for reaction. After 30 min, UV–vis measurements were performed for antioxidant quantification for each concentration of CACQDS, and changes in the absorbance were recorded at 517 nm. A graph was plotted for absorbance as a function of CACQDs concentration.

The percentage scavenging activity from recorded absorbance values were calculated using the following formula,

$$\%\ Antioxidant\ \ Activity = \frac{Absorbance\ \ of\ \ DPPH\ \ -\ \ Absorbance\ \ of\ \ Sample}{Absorbance\ \ of\ \ DPPH}$$

2.9. Fibril inhibition ThT assay

Lysozyme fibrils were prepared by dissolving 3 mg/mL (139 μM) of lysozyme in the buffer of 20 mM KH_2PO_4 and 3 M guanidine hydrochloride. CACQD solutions were prepared at different concentrations and added to individual treatment vials. Vials were incubated at 60 °C, 500 rpm for 4 h using an incubator shaker (Multi-therm, Benchmark). After 5h, fibril formation was observed in vials. In a quartz cuvette, 20 μM ThT was added to the lysozyme after 10 s and fluorescence intensity was measured for 120 s using a DM45 Olis spectrofluorometer. The measurements were recorded by exciting samples at 450 nm, and emission was observed at 482 nm at a constant integration time of 0.1 s.

2.10. In vitro cytotoxicity and neuroprotective efficacy of CACQDS

The SH-SY5Y cells were revived and maintained in freshly prepared DMEM/F-12 media at 37 °C under 5% carbon dioxide (CO_2). Once they attained 70% confluency, cells were treated with trypsin and re-suspended in fresh media. Cells were then counted and seeded in 96-well plates at a cell-density of 10,000 cells/well. Cells were incubated for 12 h to settle down and gain morphology. The experiment included untreated cells as the negative control and hydrogen peroxide-treated cells (10 mM H_2O_2) as a positive control. Cells were treated with different concentrations of CACQDs followed by 24 h incubation. After 24 h incubation, cells were stained with Hoechst/PI (1 μg/mL) by adding 10 μL/well, followed by 1h of incubation before the cytotoxicity measurements. The cytotoxicity analysis was performed using a multi-plate reader (IN Cell Analyzer, 2000 Bioimager, GE

HEALTHCARE). The data provides the % cell death as a function of CACQD treatments at different concentrations.

Using Hemocytometer cells were counted and 10,000 cells/well were seeded into a 96-well plate to investigate the neuroprotective efficacy of CACQDs. The plate was then kept in a cell incubator for 6 h. The plate was then placed in a cell incubator and maintained for 6 h. Cells were then pre-incubated with various concentrations of CACQDs for 12 h, followed by PQ treatment, and incubated for 24 h. After 24 h, cells were stained by a similar method discussed above, and cytotoxicity measurements were performed using a multi-plate reader (IN Cell Analyser, 2000 Bioimager, GE HEALTHCARE). The data obtained were plotted, and statistical significance was demonstrated in graphs. The confocal microscopic images were captured and saved using LSM700 confocal microscope for all the treatment categories.

2.11. Statistical analysis

All data were measured in triplicate. The Statistical analysis was performed using Two-way analysis of variance (ANOVA), followed by multiple unpaired t-tests to evidence the statistical significance of variances in treatment and control samples; for identification of significant differences between two groups, p-value was determined and displayed in graphical representations.

3. Results and discussion

3.1. Physicochemical characterization of caffeic acid quantum dots

CACQDs were synthesized from caffeic acid using the green-synthesis-based hydrothermal method(Yao, M.-M. Zhao, et al., 2022). CACQDs were characterized by some spectroscopic tools. Fig. 1 (a) reflects the average hydrodynamic size of the synthesized CACQDS. A value of 8.5 nm agrees with the literature for CQDs, which range in size from 2 to 20 nm(Bera et al., 2010; Kalkal et al., 2020). Note that the length measured in DLS is hydrodynamic and slightly larger than the actual size. The polydispersity index (PDI) of CACQDS was found to be 0.3, which suggests a relatively monodisperse system. Note that PDI values range between 0.0 and 1.0. The lower limit reflects a perfectly uniform particle-sized sample while the latter value is indicative of a sample that is highly heterogeneous with respect to sample size. The monodisperse system contributes to the stability and homogeneous property of CQDs in their colloidal state. The Zeta potential measurements of CACQDs revealed a single peak at −14.9 mV (Fig. 1 (b)). The negative zeta potential value underscores the existence of negatively charged moieties on the CACQD surface which facilitate the dispersion of CACQDs in water(Radchanka et al., 2022). The negative zeta potential values in this range are indicative of the stability of the CQDs in the colloidal system.

The UV–vis spectroscopy of caffeic acid shows two distinct and relatively broad peaks at 289 nm and 314 nm (Fig. 1(c)). By contrast, recarbonization into CACQDs results in a single absorption peak at 286 nm, shown in Fig. 1 (c). While the $n \rightarrow \pi^*$ electronic transition of C=O is responsible for the absorption peak at 289 nm and 286 nm, the $\pi \rightarrow \pi^*$

electronic transition is ascribed to the absorption at 314 nm(Catauro et al., 2020). To the naked eye, CACQDs appear pale yellow under white light and display a bluish tinge when illuminated by UV light (inset to (Fig. 1 (c)). Fig. 1(d) depicts ATR-IR spectra that compares the functional groups present in the CACQDs with that in caffeic acid. These include (C–OH), (C–H), (C=C), and (C=O) in the CACQDs. A comparison of the IR spectra pre- and post-recarbonization suggests that presence of functional groups is common even after the hydrothermal treatment of the carbon source. This finding may become important for BBB penetration. The excitation-dependent emission fluorescence spectra were recorded for CACQDs. A sweep of the excitation wavelength from 280 to 380 nm resulted in a red shift of the emission (Fig. 1 (e). The data suggests the presence of multiple chemical moieties possessing distinct excitation maxima and likely defect centers in the CACQDs. The contour plot reveals an intense emission maximum when the nanomaterial is excited around 330 nm (Fig. 1 (f)). This suggests that even though the excitation maximum of the CACQDs, as evidenced from the absorption spectrum, is at 286 nm, the presence of sp^2-hybridized centers (evident from absorption at longer wavelengths) upon recarbonization of caffeic acid.

In summary, the characterization of the CQDs revealed a relatively narrow distribution of sizes which likely results from the negative and polar surface-groups present on the CACQDs. These were confirmed by IR via the presence of electron-withdrawing oxygen groups. Furthermore, the sp^2-hybridized carbon network present in CACQDs is beneficial for free-radical scavenging ability.

3.2. Antioxidant property determination by DPPH assay

DPPH is a colorimetric free radical scavenging assay by which the antioxidant properties of CACQDs were examined by its ability to neutralize diphenylpicryl hydradzyl. In the presence of antioxidants, DPPH exhibits a color change from purple to yellow, indicating the quenching of free radicals. A concentration-dependent decrease in absorbance was observed at 517 nm for treated groups compared to the control containing DPH alone. Ascorbic acid was the positive control (Fig. 2(a)). The Inset of Fig. 2(a) shows a change in color gradient upon an increase in CACQDs concentrations from left to right, from purple to yellow. A plot of the radical scavenging activity as a function of CACQDs dose is shown in Fig. 2(b). At ~100 μg/mL, nearly 100% radical scavenging was realized. These results indicate that CACQDs exhibited excellent antioxidant properties in the microgram range, indicating their potential to intervene in oxidative stress-associated disorders.

3.3. ThT assay

Proteins can misfold due to mutations, translational errors, and upon exposure to environmental toxicants, to form highly ordered aggregates of cross beta-sheet fibrils(Prabhu and Sarkar, 2022; Lin and Beal, 2006; Dobson, 2003). Amyloid formation is correlated to most neurodegenerative disorders such as Alzheimer’s disease, Parkinson’s disease, and Huntington’s disease(Prabhu and Sarkar, 2022). In this study, using HEWL as a model, we have examined the potential interventional role of CACQDs in the soluble-to-toxic transformation of amyloid-forming proteins. In control experiments, the presence of synthesized mature HEWL fibrils was confirmed by introducing ThT. The increase in

the emission intensity is indicative of its binding to the cross-beta structure in fibrils. We then investigated the dose-dependent ability of CACQDs to inhibit the soluble-to-fibril transformation of monomeric HEWL into a fibrillary structure was investigated. Varying concentrations of CACQDs challenged the HEWL fibril-forming process. The data (including untreated control (Fig. 3),) demonstrates a CACQD dose-dependent decrease in ThT fluorescence intensity. Even at an initial CACQD concentration of 1 mg/mL, there was a significant diminution in ThT fluorescence intensity, suggesting potent inhibition of fibril formation. A 5 mg/mL CACQD dose almost completely eliminated the conversion of HEWL from forming fibrils.

The data are important because the soluble-to-toxic transformation of amyloid-forming proteins is associated with the onset and pathogenesis of neurodegenerative and non-neurodegenerative disorders such a. systemic amyloidosis (HEWL), AD (amyloid-β), PD (α-synuclein) and HD (mutant HTT). Therefore, considering that CACQDs interfere in this phenomenon as demonstrated using HEWL, they are likely to have an important biomedical contribution. These data necessitate further testing in a vertebrate model of neurodegeneration.

3.4. Cellular cytotoxicity of CACQDS, dose-dependent cytotoxicity of paraquat

To determine whether CACQDs can be used safely in biological systems, we established the cytotoxicity profile of CACQDS in Human Neuroblastoma cell line (SHSY–5Y). The data indicates that CACQDs up to 5 mg/mL tested concentration did not elicit cytotoxicity more significantly than untreated and vehicle controls (Fig. 4(a)). By contrast, as anticipated, paraquat insult to the cell line elicited a dose-dependent cytotoxic response at concentrations >500 μM (Fig. 4(b)). In both sets of experiments, hydrogen peroxide served as a positive control.

3.5. Cell rescue from paraquat toxicity

We determined whether cells preincubated with CACQDS could prevent paraquat-induced cell death, which is important considering that exposure to the neurotoxin initiates dopaminergic injury and demise(Sinclair et al., 2021). As shown in Fig. 5, PQ concentrations >500 μM were found to be cytotoxic with 5 mM paraquat leading to 50% cell death. Hence, a 5 mM concentration was chosen for further investigation. SH-SY5Y cells were treated with PQ (5 mM) after preincubation with different concentrations of CACQDs. A concentration of 5 mg/mL CACQDs significantly reduced cell death (by ~45%). When CACQD levels were reduced to 3 mg/mL, cell death was also significantly reduced (20%) (Fig. 6(a)). At 0.1 mg/mL concentration of CACQDs, cell death inhibition was ~15%. Preincubation of the cell line with CACQDs at 0.01 mg/mL was found to have a statistically insignificant impact on paraquat-induced cell death (Fig. 6(a)). These data suggest that CACQDS are successfully capable of mitigating oxidative stress-induced cell death by paraquat.

Furthermore, confocal microscopy of neuroblastoma cells was performed for all group cell rescue experiments (Fig. 6(b)). Cells were stained with Hoechst and PI to differentiate between live and dead cells (Lema et al., 2011). A concentration-dependent decrease in dead

cells was observed in treatment groups from 1 mg/mL to 5 mg/mL, as depicted in Fig. 6(b). In contrast, only a few cells were found dead in Untreated wells, and nearly all were found dead in H_2O_2-treated cells (positive control). The confocal microscopic images strongly correlate with the cell rescue data obtained from cytotoxicity analysis.

The results from Sections 3.4 and 3.5 are biologically relevant. They not only speak to the biocompatible nature of CACCQDs but also reveal that CACDQs are able to mitigate paraquat-associated cellular dyshomeostasis in vivo.

4. Conclusions

Neurodegenerative diseases result from many pathological conditions, including oxidative stress, aging, genetic disorders, and exposure to toxic environmental chemicals such as pesticides. The soluble-to-toxic transformation of amyloid-forming proteins is a cardinal feature of PD, AD, HD, and other neurodegenerative disorders. Second, elevated levels of ROS resulting in neuronal dyshomeostasis, injury, and demise drive neurodegeneration. In the laboratory, the herbicide paraquat is commonly used to mimic the onset and progress of PD. Exposure of dopaminergic neurons to the neurotoxicant paraquat leads to oxidative stress, amyloid aggregation, dopaminergic neuronal injury, neuronal demise, and PD pathology. Here, we investigated the neuroprotective efficacy of caffeic acid-based quantum dots via hydrothermal synthesis against the soluble-to-toxic aggregation of an amyloid protein and against paraquat-driven ROS elevation. Our data suggest that CACQDs intervene in the formation of HEWL fibrils by preventing the soluble-to-toxic transformation of monomeric HEWL. Separately, CACQDs mitigate cell mortality arising from paraquat-induced elevation in ROS. These, as aforementioned, are independent milestones along the trajectories to a host of neurodegenerative disorders, including PD, AD and HD. It is worth noting that against both aberrant factors, CACQD intervention was dose-dependent. Importantly, the use of bio-waste (coffee grinds) derived CACQDs are able to mitigate neurotoxic outcomes associated with an environmentally widely used pesticide. Our data position this green chemistry synthesis-derived sustainable nanomaterial for preclinical trials involving vertebrate models of neurodegenerative pathology that will include studies designed to examine the potential of CACQDs to cross the BBB.

Acknowledgments

The authors are grateful to the National Institute of General Medical Sciences of the National Institutes of Health (NIH/NIGMS) under Award Number 1R16GM145575–01 for supporting this work. We thank Dr. Armando Varela, Gladys Almodovar, Denisse A Gutierrez. We are also thankful to all the staff members of the cellular Characterization and Biorepository Core facility, Border Biomedical Research Center, the University of Texas at El Paso (UTEP). The facility is supported by the National Institute of Health (NIH) and National Institute of Mental Health (NIMH) grants # 2G12MD007592, 5U54MD007592, and 5G12MD007592. We sincerely thank Dr. Jorge Gardea-Torresdey for helping in Dynamic Light Scattering measurements.

Data availability

Data will be made available on request.

References

Agarwal A, et al. , 2009. Nanoparticles as novel carrier for brain delivery: a review. Curr. Pharmaceut. Des. 15 (8), 917–925. 10.2174/138161209787582057.

Alam M, et al. , 2022. Therapeutic implications of caffeic acid in cancer and neurological diseases. Front. Oncol. 12 10.3389/FONC.2022.860508.

Alizadeh S, et al. , 2022. Paraquat induced oxidative stress, DNA damage, and cytotoxicity in lymphocytes. Heliyon 8 (7). 10.1016/J.HELIYON.2022.E09895.

Bai J, et al., 2021. Biomineral calcium-ion-mediated conductive hydrogels with high stretchability and self-adhesiveness for sensitive iontronic sensors Highlights Transparent and highly ionic-conductive hydrogels utilizing Ca 2+ 10.1016/j.xcrp.2021.100623.

Banerjee R, Kaidery NA, Thomas B, 2015. Oxidative stress in Parkinson's disease: role in neurodegeneration and targets for therapeutics. In: Oxidative Stress: Diagnostics, Prevention, and Therapy, vol. 2. American Chemical Society (ACS Symposium Series), pp. 147–176. 10.1021/bk-2015-1200.ch005. SE–5.

Begley DJ, 2004. Delivery of therapeutic agents to the central nervous system: the problems and the possibilities. Pharmacol. Therapeut. 104 (1), 29–45. 10.1016/J.PHARMTHERA.2004.08.001.

Bera D, et al. , 2010. Quantum dots and their multimodal applications: a review. Materials 3 (4), 2260. 10.3390/MA3042260.

Blesa J, et al. , 2015. Oxidative stress and Parkinson's disease. Front. Neuroanat. 9, 91. 10.3389/fnana.2015.00091. [PubMed: 26217195]

Cal M, Szakonyi Z, Pavlíková N, 2022. Caffeic acid and diseases__mechanisms of action. Int. J. Mol. Sci. 24 (1), 588. 10.3390/IJMS24010588, 2023. [PubMed: 36614030]

Catauro M, et al. , 2020. New SiO2/Caffeic acid hybrid materials: synthesis, spectroscopic characterization, and bioactivity. Materials 13 (2). 10.3390/MA13020394.

Chen JH, Ho CT, 1997. Antioxidant activities of caffeic acid and its related hydroxycinnamic acid compounds. J. Agric. Food Chem. 45 (7), 2374–2378. 10.1021/JF970055T.

Cheng Guowang, et al. , 2022. Anti-parkinsonian therapy: strategies for crossing the blood–brain barrier and nano-biological effects of nanomaterials. Nano-Micro Lett. 14 10.1007/S40820-022-00847-Z.

Chitnis T, Weiner HL, 2017. CNS inflammation and neurodegeneration. J. Clin. Investig. 127 (10), 3577–3587. 10.1172/JCI90609. [PubMed: 28872464]

Corasaniti MT, et al. , 1992. Neurotoxic effects induced by intracerebral and systemic injection of paraquat in rats. Hum. Exp. Toxicol. 11 (6), 535–539. 10.1177/096032719201100616. [PubMed: 1361145]

Cui W, et al. , 2021. Application of nanomaterials in neurodegenerative diseases. Curr. Stem Cell Res. Ther. 16 (1), 83–94. 10.2174/1574888X15666200326093410. [PubMed: 32213159]

Deshmukh RS, Chaudhary RK, Roy I, 2012. Effect of pesticides on the aggregation of mutant huntingtin protein. Mol. Neurobiol. 45 (3), 405–414. 10.1007/S12035-012-8252-2. [PubMed: 22415443]

Dobson CM, 2003. Protein folding and misfolding. Nature 426 (6968), 884–890. 10.1038/NATURE02261. [PubMed: 14685248]

Dorsey ER, Ray A, 2023. Paraquat, Parkinson's disease, and agnotology. Mov. Disord. 10.1002/MDS.29371.

Dugger BN, Dickson DW, 2017. Pathology of neurodegenerative diseases. Cold Spring Harbor Perspect. Biol. 9 (7) 10.1101/cshperspect.a028035.

El-Seedi HR, et al. , 2012. Biosynthesis, natural sources, dietary intake, pharmacokinetic properties, and biological activities of hydroxycinnamic acids. J. Agric. Food Chem. 60 (44), 10877–10895. 10.1021/JF301807G. [PubMed: 22931195]

Grabska-Kobylecka I, et al. , 2020. The presence of caffeic acid in cerebrospinal Fluid: evidence that dietary polyphenols can cross the blood-brain barrier in humans. Nutrients 12 (5). 10.3390/NU12051531.

Henriquez G, et al. , 2022. Citric acid-derived carbon quantum dots attenuate paraquat-induced neuronal compromise in vitro and in vivo. ACS Chem. Neurosci. 13 (16), 2399–2409. 10.1021/acschemneuro.2c00099. [PubMed: 35942850]

Hernandez LF, Redgrave P, Obeso JA, 2015. Habitual behavior and dopamine cell vulnerability in Parkinson disease. Front. Neuroanat. 9 10.3389/FNANA.2015.00099. AUGUST.

Hwang JY, et al. , 2013. Biofunctionalized carbon nanotubes in neural regeneration: a mini-review. Nanoscale 5 (2), 487–497. 10.1039/C2NR31581E. [PubMed: 23223857]

Janus Ł, et al. , 2020. Smart, tunable CQDs with antioxidant properties for biomedical applications—ecofriendly synthesis and characterization. Molecules 25 (3). 10.3390/MOLECULES25030736.

Jung H, et al. , 2022. Recent progress on carbon quantum dots based photocatalysis. Front. Chem. 10, 881495 10.3389/FCHEM.2022.881495/BIBTEX. [PubMed: 35548671]

Jung L, et al. , 2020. Untangling the potential of carbon quantum dots in neurodegenerative disease. Processes 8 (5), 599. 10.3390/PR8050599.

Kalkal A, et al. , 2020. Biofunctionalized graphene quantum dots based fluorescent biosensor toward efficient detection of small cell lung cancer. ACS Appl. Bio Mater. 3 (8), 4922–4932. 10.1021/ACSABM.0C00427.

Kreuter J, 2004. Influence of the surface properties on nanoparticle-mediated transport of drugs to the brain. J. Nanosci. Nanotechnol. 4 (5), 484–488. 10.1166/JNN.2003.077. [PubMed: 15503433]

Lamptey RNL, et al. , 2022. A review of the common neurodegenerative disorders: current therapeutic approaches and the potential role of nanotherapeutics. Int. J. Mol. Sci. 23 (3) 10.3390/ijms23031851.

Lema C, Varela-Ramirez A, Aguilera RJ, 2011. Differential nuclear staining assay for high-throughput screening to identify cytotoxic compounds. Curr. Cell. Biochem. 1 (1), 1–14. [PubMed: 27042697]

Lim SY, Shen W, Gao Z, 2014. Carbon quantum dots and their applications. Chem. Soc. Rev. 44 (1), 362–381. 10.1039/C4CS00269E. [PubMed: 25316556]

Lim SY, Shen W, Gao Z, 2015. Carbon quantum dots and their applications. Chem. Soc. Rev. 44 (1), 362–381. 10.1039/C4CS00269E. [PubMed: 25316556]

Lin MT, Beal MF, 2006. Mitochondrial dysfunction and oxidative stress in neurodegenerative diseases. Nature 443 (7113), 787–795. 10.1038/NATURE05292. [PubMed: 17051205]

McCormack AL, et al. , 2005. Role of oxidative stress in paraquat-induced dopaminergic cell degeneration. J. Neurochem. 93 (4), 1030–1037. 10.1111/J.1471-4159.2005.03088.X. [PubMed: 15857406]

Miller G, 2002. Drug targeting. Breaking down barriers. Science (New York, N.Y.) 297 (5584), 1116–1118. 10.1126/SCIENCE.297.5584.1116. [PubMed: 12183610]

Miller GW, 2007. Paraquat: the red herring of Parkinson's disease research. Toxicol. Sci. : Off. J. Soc. Toxicol. 100 (1), 1–2. 10.1093/TOXSCI/KFM223.

Mirzaei S, et al. , 2021. Caffeic acid and its derivatives as potential modulators of oncogenic molecular pathways: new hope in the fight against cancer. Pharmacol. Res. 171 10.1016/J.PHRS.2021.105759.

Mishra R, et al. , 2007. Lysozyme amyloidogenesis is accelerated by specific nicking and fragmentation but decelerated by intact protein binding and conversion. J. Mol. Biol. 366 (3), 1029–1044. 10.1016/J.JMB.2006.11.084. [PubMed: 17196616]

Modi G, et al. , 2009. Nanotechnological applications for the treatment of neurodegenerative disorders. Prog. Neurobiol. 88 (4), 272–285. 10.1016/j.pneurobio.2009.05.002. [PubMed: 19486920]

Modi P, et al. , 2016. 'Understanding Pathophysiology of Sporadic Parkinson's Disease in Drosophila Model: Potential Opportunities and Notable Limitations', Challenges in Parkinson's Disease. 10.5772/63767.

Mohanraj K, Sethuraman S, Krishnan UM, 2013. Development of poly(butylene succinate) microspheres for delivery of levodopa in the treatment of Parkinson's disease. J. Biomed. Mater. Res. B Appl. Biomater. 101 (5), 840–847. 10.1002/JBM.B.32888. [PubMed: 23401377]

Molaei MJ, 2019. Carbon quantum dots and their biomedical and therapeutic applications: a review. RSC Adv. 9 (12), 6460. 10.1039/C8RA08088G. [PubMed: 35518468]

Di Monte DA, Lavasani M, Manning-Bog AB, 2002. Environmental factors in Parkinson's disease. Neurotoxicology 23 (4–5), 487–502. 10.1016/S0161-813X(02)00099-2. [PubMed: 12428721]

Monteiro Espíndola KM, et al. , 2019. Chemical and pharmacological aspects of caffeic acid and its activity in Hepatocarcinoma. Front. Oncol. 9, 541. 10.3389/FONC.2019.00541. JUN. [PubMed: 31293975]

Namdari P, Negahdari B, Eatemadi A, 2017. Synthesis, properties and biomedical applications of carbon-based quantum dots: an updated review. Biomedicine & pharmacotherapy = Biomedecine & pharmacotherapie 87, 209–222. 10.1016/J.BIOPHA.2016.12.108. [PubMed: 28061404]

Nandipati S, Litvan I, 2016. Environmental exposures and Parkinson's disease. Int. J. Environ. Res. Publ. Health 13 (9). 10.3390/IJERPH13090881.

Papapetropoulos S, et al. , 2001. Clinical phenotype in patients with α-synuclein Parkinson'sdisease living in Greece in comparison with patients with sporadicParkinson's disease. J. Neurol. Neurosurg. Psychiatr. 70 (5), 662. 10.1136/JNNP.70.5.662.

Poovaiah N, et al. , 2018a. Treatment of neurodegenerative disorders through the blood-brain barrier using nanocarriers. Nanoscale 10 (36), 16962–16983. 10.1039/c8nr04073g. [PubMed: 30182106]

Poovaiah N, et al. , 2018b. Treatment of neurodegenerative disorders through the blood–brain barrier using nanocarriers. Nanoscale 10 (36), 16962–16983. 10.1039/C8NR04073G. [PubMed: 30182106]

Prabhu MPT, Sarkar N, 2022. Inhibitory effects of carbon quantum dots towards hen egg white lysozyme amyloidogenesis through formation of a stable protein complex. Biophys. Chem. 280 10.1016/J.BPC.2021.106714.

Radchanka A, et al. , 2022. Zeta potential-based control of CdSe/ZnS quantum dot photoluminescence. J. Phys. Chem. Lett. 13 (22), 4912–4917. 10.1021/acs.jpclett.2c00841. [PubMed: 35634986]

Saito N, et al. , 2009. Carbon nanotubes: biomaterial applications. Chem. Soc. Rev. 38 (7), 1897–1903. 10.1039/b804822n. [PubMed: 19551170]

Sartori F, Vidrio E, 2018. Environmental fate and ecotoxicology of paraquat: a California perspective 100 (5–7), 479–517. 10.1080/02772248.2018.1460369.

Scalbert A, et al. , 2005. Dietary polyphenols and the prevention of diseases. Crit. Rev. Food Sci. Nutr. 45 (4), 287–306. 10.1080/1040869059096. [PubMed: 16047496]

Silva T, Oliveira C, Borges F, 2014. Caffeic acid derivatives, analogs and applications: a patent review (2009–2013). Expert Opin. Ther. Pat. 24 (11), 1257–1270. 10.1517/13543776.2014.959492. [PubMed: 25284760]

Sinclair E, et al. , 2021. Metabolomics of sebum reveals lipid dysregulation in Parkinson's disease. Nat. Commun. 12 (1), 1–9. 10.1038/s41467-021-21669-4. [PubMed: 33397941]

Singh A, et al. , 2021. Quantum dot: Heralding a brighter future in neurodegenerative disorders. J. Drug Deliv. Sci. Technol. 65, 102700 10.1016/J.JDDST.2021.102700.

Song J, et al. , 2020. Multifunctional antimicrobial biometallohydrogels based on amino acid coordinated self-assembly. Small 16 (8). 10.1002/SMLL.201907309.

Soni S, Ruhela RK, Medhi B, 2016. Nanomedicine in central nervous system (CNS) disorders: a present and future prospective. Adv. Pharmaceut. Bull. 6 (3), 319. 10.15171/APB.2016.044.

Stockwell J, et al. , 2014. Novel central nervous system drug delivery systems. Chem. Biol. Drug Des. 83 (5), 507–520. 10.1111/CBDD.12268. [PubMed: 24325540]

Sun Y-P, et al. , 2006. Quantum-sized carbon dots for bright and colorful photoluminescence. J. Am. Chem. Soc. 128 (24), 7756–7757. 10.1021/ja062677d. [PubMed: 16771487]

Suri SS, Fenniri H, Singh B, 2007. Nanotechnology-based drug delivery systems. J. Occup. Med. Toxicol. 2 (1), 1–6. 10.1186/1745-6673-2-16. [PubMed: 17261183]

Uversky VN, 2004. Neurotoxicant-induced animal models of Parkinson's disease: understanding the role of rotenone, maneb and paraquat in neurodegeneration. Cell Tissue Res. 318, 225–241. 10.1007/s00441-004-0937-z. [PubMed: 15258850]

Vaccari C, El Dib R, de Camargo JLV, 2017. Paraquat and Parkinson's disease: a systematic review protocol according to the OHAT approach for hazard identification. Syst. Rev. 6 (1) 10.1186/S13643-017-0491-X.

Warner TT, et al. , 2003. Genetic and environmental factors in the cause of Parkinson's disease. Ann. Neurol. 53 (Suppl. 3) 10.1002/ANA.10487.

Wei Z, et al. , 2018. Oxidative stress in Parkinson's disease: a systematic review and meta-analysis. Front. Mol. Neurosci. 11, 236. 10.3389/fnmol.2018.00236. [PubMed: 30026688]

Xing Ruirui, et al., 2016. An Injectable Self-Assembling Collagen-Gold Hybrid Hydrogel for Combinatorial Antitumor Photothermal/Photodynamic Therapy. 10.1002/adma.201600284.

Yan D, et al. , 2016. Pesticide exposure and risk of Alzheimer's disease: a systematic review and meta-analysis. Sci. Rep. 6 10.1038/SREP32222.

Yao L, Zhao M-M, et al. , 2022a. Carbon quantum dots-based nanozyme from coffee induces cancer cell Ferroptosis to activate antitumor immunity. ACS Nano 16 (6), 9228–9239. 10.1021/acsnano.2c01619. [PubMed: 35622408]

Yao L, Zhao MM, et al. , 2022b. Carbon quantum dots-based nanozyme from coffee induces cancer cell Ferroptosis to activate antitumor immunity. ACS Nano 16 (6), 9228–9239. 10.1021/ACSNANO.2C0161. [PubMed: 35622408]

Yi X, et al. , 2014. Agile delivery of protein therapeutics to CNS. J. Contr. Release : Off. J. Contr. Release Soc. 637. 10.1016/J.JCONREL.2014.06.017.

Younis MA, et al. , 2022. Clinical translation of nanomedicines: challenges, opportunities, and keys. Adv. Drug Deliv. Rev. 181 10.1016/J.ADDR.2021.114083.

Zhang W, et al. , 2021. Carbon dots: a future blood-brain barrier penetrating nanomedicine and drug nanocarrier. Int. J. Nanomed. 16, 5003–5016. 10.2147/IJN.S318732.

Zhang Z, et al. , 2016. Caffeic acid ameliorates colitis in association with increased Akkermansia population in the gut microbiota of mice. Oncotarget 7 (22), 31790–31799. 10.18632/ONCOTARGET.9306. [PubMed: 27177331]

Zielińska D, et al. , 2021. Caffeic acid modulates processes associated with intestinal inflammation. Nutrients 13 (2), 554. 10.3390/NU13020554. [PubMed: 33567596]

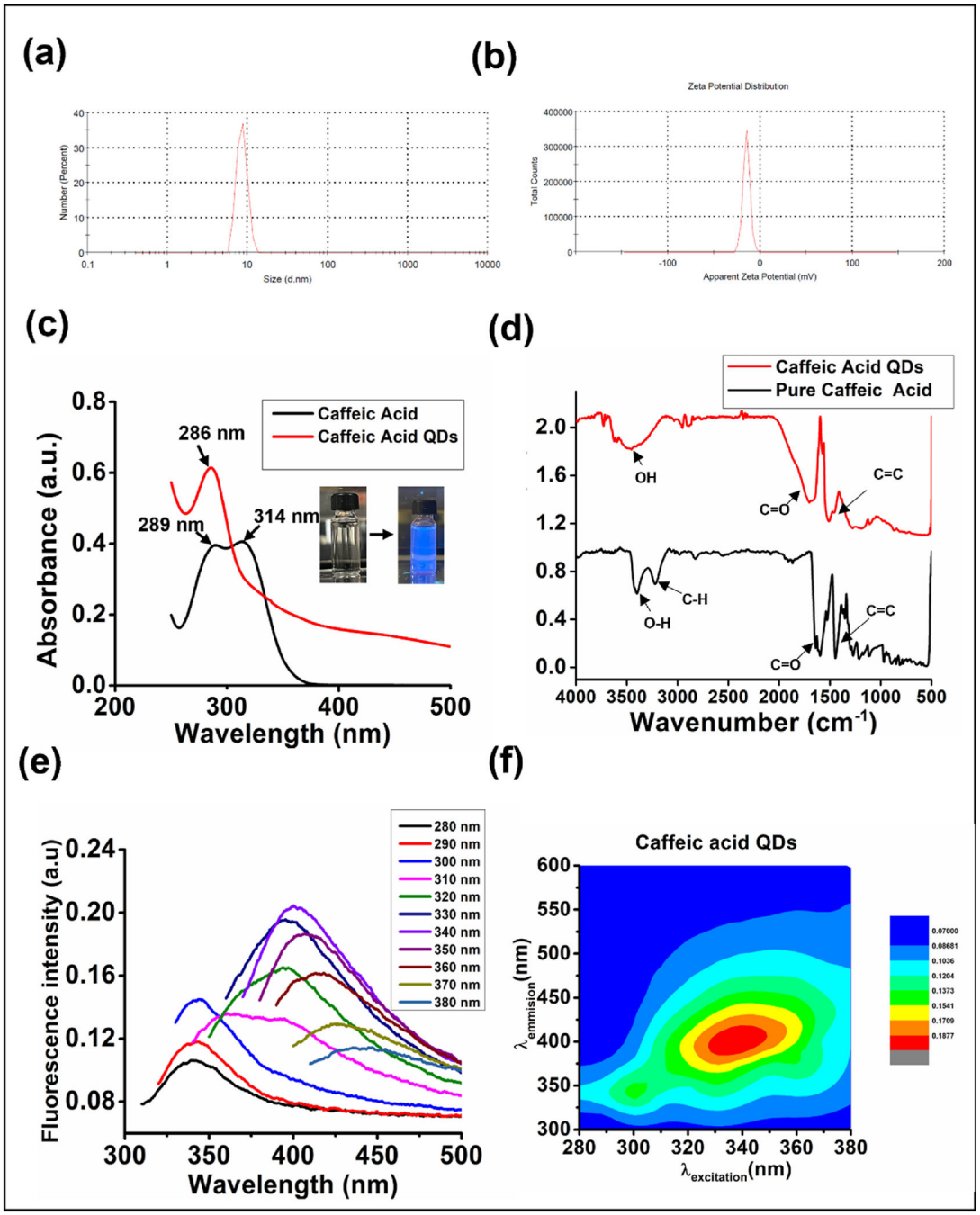

Fig. 1.

Physicochemical characterization data of CACQDs (a) Dynamic Light Scattering indicating the size-distribution of CACQDs and b) Zeta potential measurements (reflecting negative surface-charge) of CACQDs dispersed in water. (c) UV–vis absorption spectra of caffeic acid and CACQDs. Inset: Image of CACQDs under natural light (left) and UV light (right). (d) IR spectra of caffeic acid (bottom) and post-recarbonization (top) showing the transformation of functional groups (e) Excitation dependent emission spectra of CACQDs.

(f) Corresponding contour plot showing fluorescence centers as a function of excitation wavelength and uantum yield.

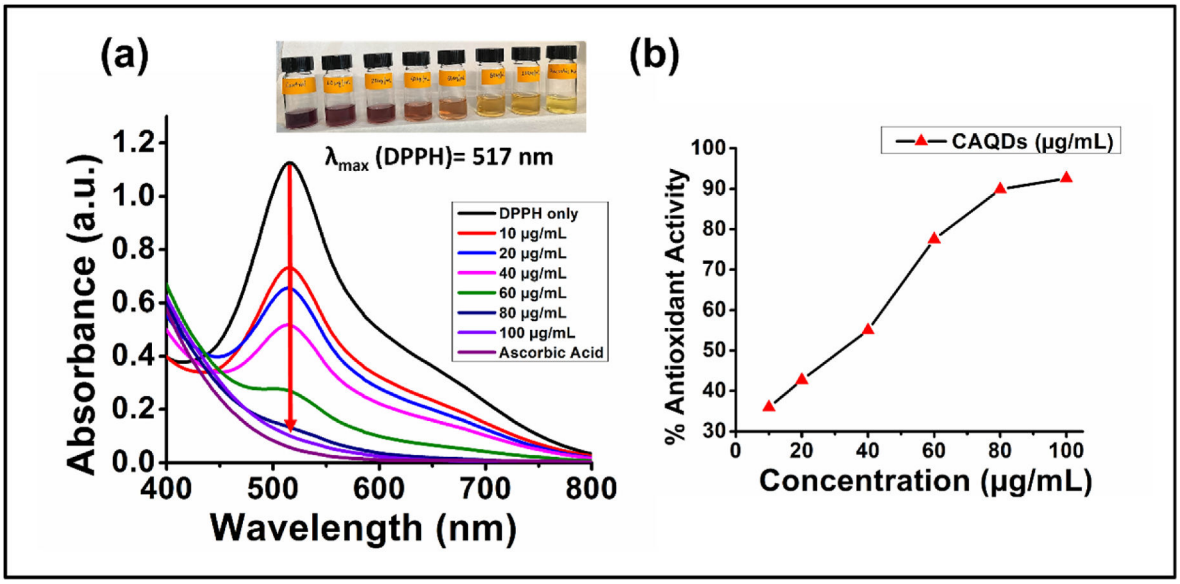

Fig. 2.

DPPH free radical Scavenging Assay. (a) Typical absorption spectra of DPPH alone and in presence of different concentration of CACQDs (10 µg/mL to 100 µg/mL). (b) A plot of percentage of antioxidant activity vs concentration of CAQDs (µg/mL).

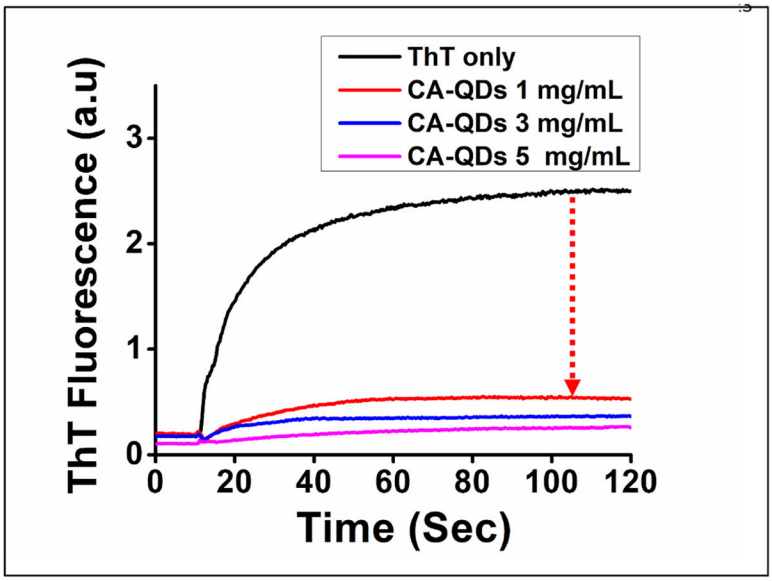

Fig. 3.

Fibrillation inhibition Assay using HEWL. (a) ThT fluorescence of HEWL as negative Control (b) Decreased ThT fluorescence of HEWL preincubated with CACQDs.

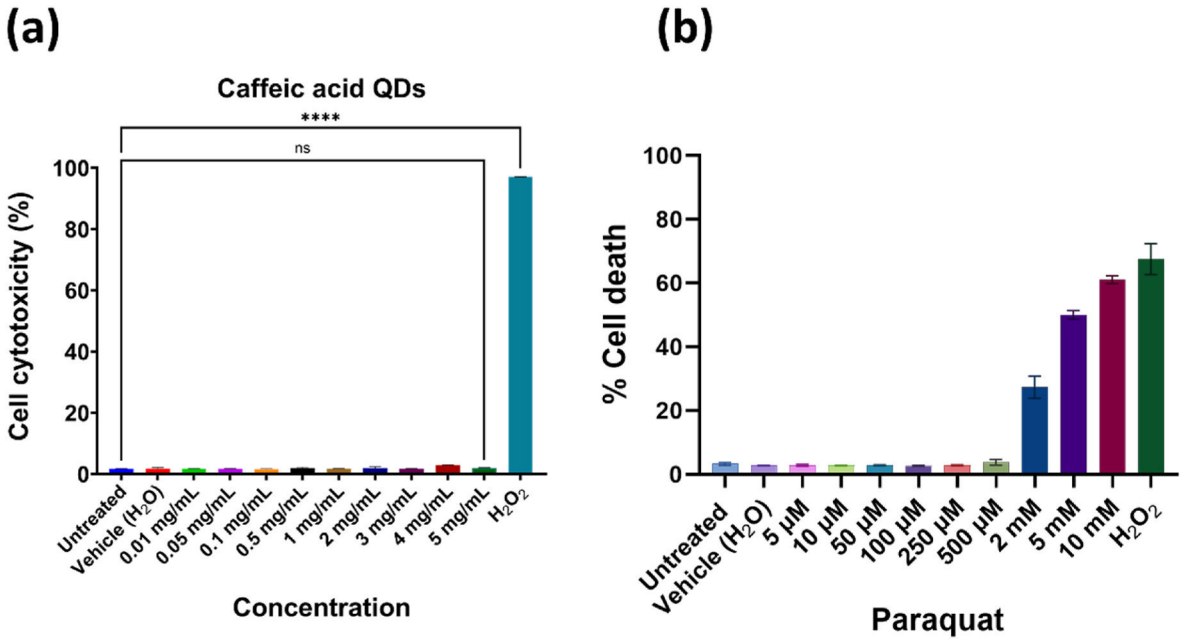

Fig. 4.

Cytotoxicity assay in SH-SY5Y cells using Hoechst and PI (a) Neuroblastoma cells treated with CACQDs at different concentrations (b) Paraquat dose-dependent cytotoxicity.

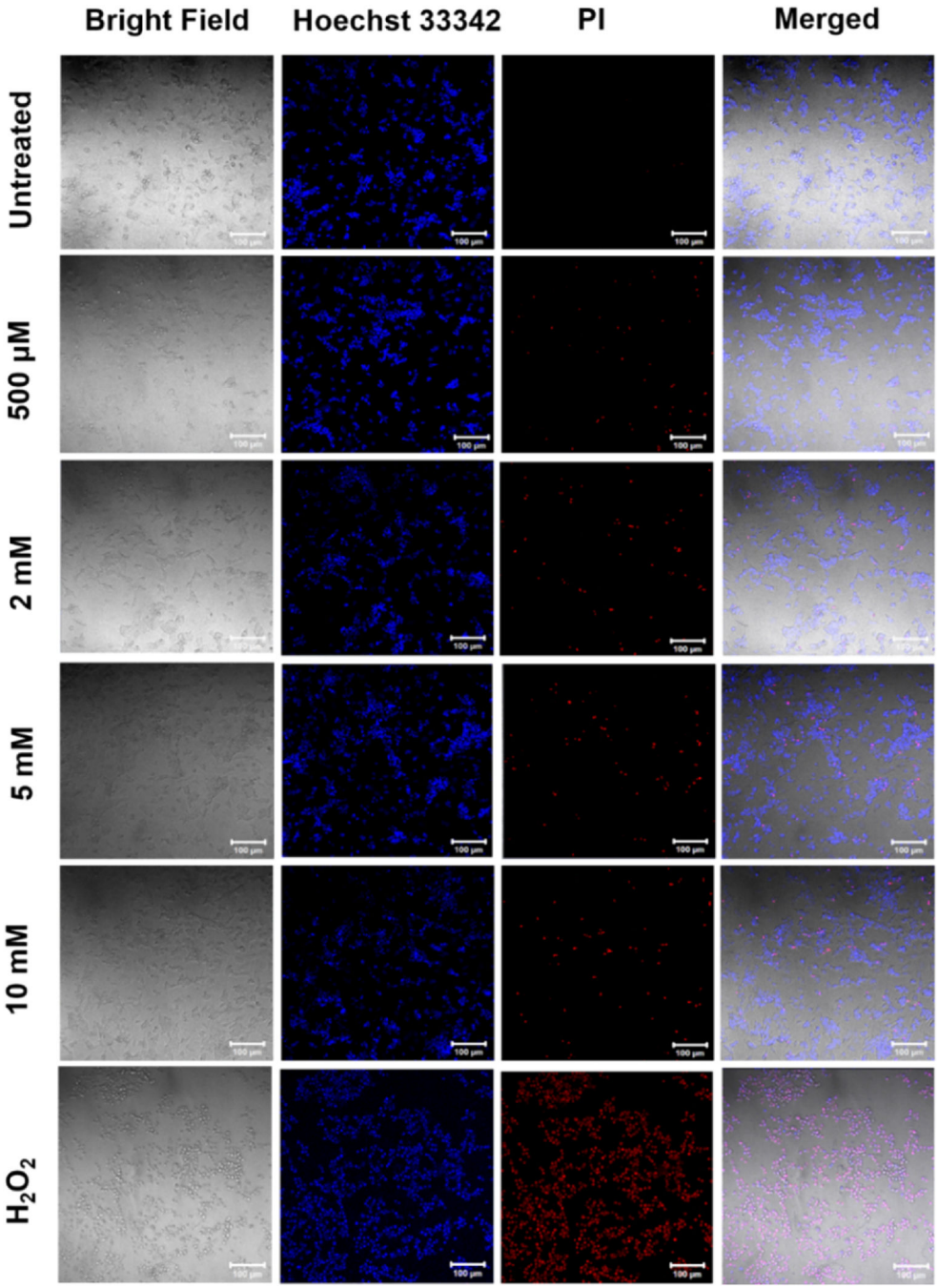

Fig. 5.

Confocal images of SH-SY5Y cells for evaluation of paraquat toxicity in Untreated cells (negative control), paraquat concentration (500 µM, 2 mM, 5 mM, 10 mM) and positive control 10 mM (H_2O_2).

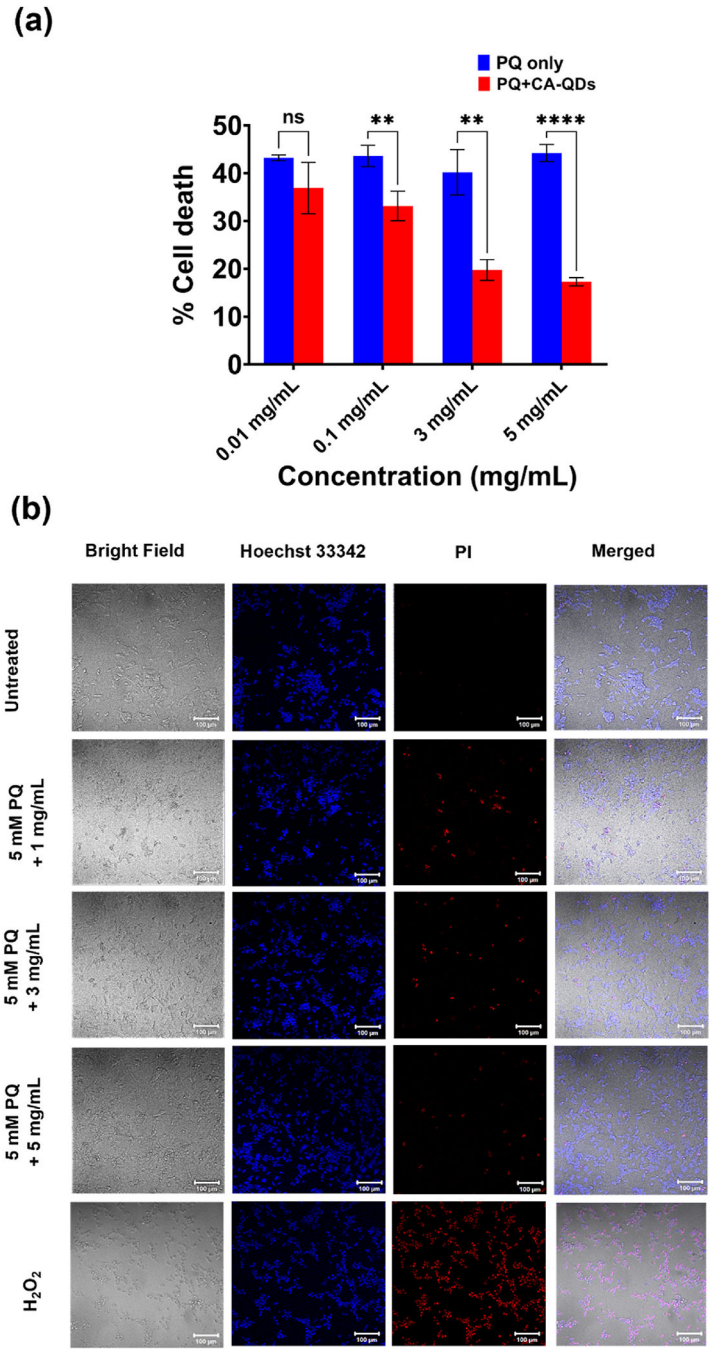

Fig. 6.

Neuroprotective efficacy of CACQDs against paraquat insult. (a) rescue of cells from Paraquat induced oxidative stress, cells pre-incubated with CAQDs followed by paraquat treatment (5 mM), rescue of cell death by different concentrations of CACQDs (b) confocal imaging of cells using Hoechst/PI showing live and dead cells in Negative control (Untreated), CACQDs treatments (0.1 mg/mL, 3 mg/mL and 5 mg/mL) and Positive control 5 mM PQ. Graphical data indicates the averages of three replicates of experiments with standard deviation values (±SD) shown in each bar. Statistical analysis were performed

using Two-way analysis of variance (ANOVA), followed by multiple unpaired t-tests. (In graph, * represent p values, where *, **and **** value indicates of $P \leq 0.05$, $P \leq 0.01$ and $P \leq 0.0001$ respectively.)

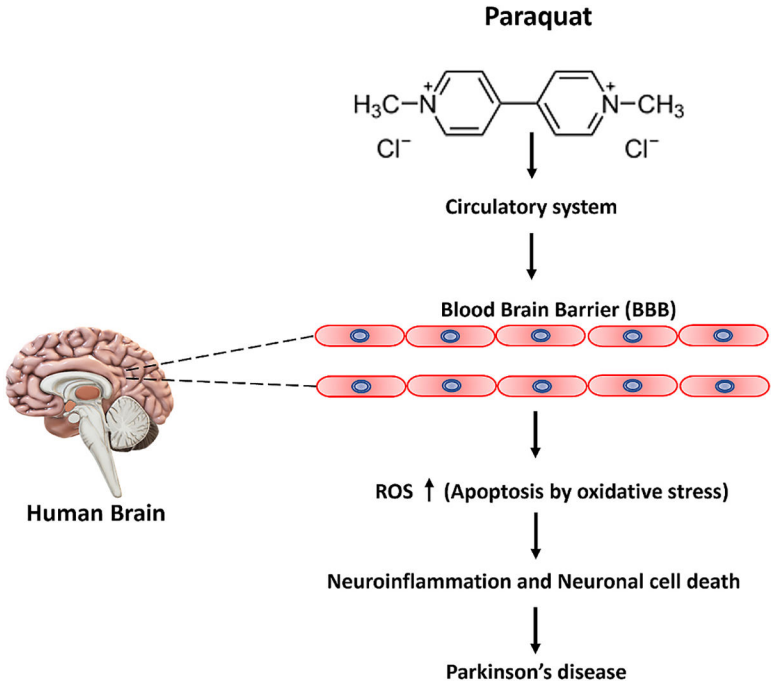

Scheme 1.

Mechanism of paraquat toxicity inducing neuronal cell death in Parkinson's disease.